space, different vehicle orientations can be well identified and analyzed.

3. Vehicle description

Object representation is an essential task in object detection and identification. In what follows, we propose a novel vehicle descriptor combining vehicle color and edge map for vehicle orientation clustering.

3.1 Vehicle Color Descriptor

This paper introduce a new color transformation for transforming all pixels with (R, G, B) colors to a new domain. Then, a specific "vehicle color" can be found and defined for effective vehicle orientation detection. Thousands of training images, including roads parking spaces, building and natural scenes, are first collected from different scenes. Through a statistic analysis, we can get the covariance matrix $\sum$ of the color distributions of *R*, *G*, and *B* from these *N* images. Using the Karhunen-Loeve transform, the eigenvectors and eigenvalues of $\sum$ can be further obtained and represented as e_i and λ_i, respectively, for *i* = 1, 2, and 3. Then, three new color features C_i can be formed and defined, respectively,

$$C_i = e_i^r R + e_i^g G + e_i^b B \text{ for } i=1, 2, \text{ and } 3, \quad (1)$$

where $e_i = (e_i^r, e_i^g, e_i^b)$. The color feature C_1 with the largest eigenvalue is

$$C_1 = \frac{1}{3}R + \frac{1}{3}G + \frac{1}{3}B . \quad (2)$$

Then, we use two other eigenvectors to form a new color plane (u,v) perpendicular to the axis $(1/3,1/3,1/3)$. The vehicle color descriptor equation is represented as:

$$u_p = \frac{2Z_p - G_p - B_p}{Z_p}, \quad v_p = \left\{ \frac{Z_p - G_p}{Z_p}, \frac{Z_p - B_p}{Z_p} \right\}, \quad (3)$$

where (R_p, G_p, B_p) is the color pixel of p and $Z_p = (R_p + G_p + B_p)/3$ is used for normalization. If we project all the vehicle pixels to the (*u*, *v*) plane, all of them will concentrate around a small circle. Then, the problem of vehicle color detection becomes a 2-class separation problem which tries to find a best decision boundary from the (*u, v*) space such that all vehicle pixels can be well separated from the non-vehicle class. In order to accurately identify vehicle pixels, in what follows, a Bayesian classifier is designed.

Assume that m_v and $m_{\sim v}$ are the means of vehicle color and non-vehicle pixels respectively obtained from the training images in the (u,v) domain, $\sum_v$ and $\sum_{\sim v}$ are their corresponding covariance matrices in the same color domain. Given a pixel x, the probability belonging to a vehicle pixel or non-vehicle pixel is based on the following equations,

$$p(x \mid v) = \left|2\pi \sum\nolimits_v\right|^{-1/2} \exp(-d_v(x)), \quad (4)$$

and

$$p(x \mid \sim v) = \left|2\pi \sum\nolimits_{\sim v}\right|^{-1/2} \exp(-d_{\sim v}(x)), \quad (5)$$

where $d_v(x) = (x - m_v)\sum_v^{-1}(x - m_v)^t / 2$ and $d_{\sim v}(x) = (x - m_{\sim v})\sum_{\sim v}^{-1}(x - m_{\sim v})^t / 2$. The pixel is regarded as a vehicle color if

$$p(x \mid v)P(v) > p(x \mid \sim v)P(\sim v), \quad (6)$$

where $P(v)$ and $P(\sim v)$ are the priori class probabilities of vehicle and non-vehicle pixels. Making use of Eqs. (4) and (5) into (6), the decision rules is: A pixel belongs to "vehicle " if

$$d_{\sim v}(x) - d_v(x) > \lambda , \quad (7)$$

where $\lambda = \log[\sqrt{\sum_v \sum_{\sim v}^{-1}} \frac{P(\sim v)}{P(v)}]$.

3.1.1 Vehicle Color Distribution

(a) (b)

Figure 2: Vehicle color detection: (a) Input image. (b) Result of vehicle color detection.

After performing the method mentioned above, the vehicle color can be detected as the result in Figure 2. The log-polar histogram is adopted to describe a vehicle color image, which is similar to the one mention in the shape context [13].

Figure 3: Log-polar location gird.

Like Figure 3, the log-polar location grid with twenty-four location bins is applied, and each one includes three bins for radial direction and eight bins in angular direction. The log-polar location gird is applied in the query image where the core of the gird is the center of the query image. We calculate the amount of the vehicle color points in each bin, and the vehicle color histogram descriptor is obtained from this step.

3.1.2 Vehicle Color Orientation

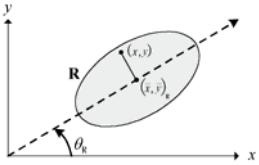

Figure 4: The gravity center $(\bar{x}, \bar{y})_R$ and orientation θ_R of a region *R*.

In addition to color distribution, the orientation of vehicle color region will also form a useful feature for vehicle orientation classification. Assume that *R* is the vehicle region. The central moments of *R* can be defined as

$$(\mu_{p,q})_R = \sum_{(x,y)\in R} (x - \bar{x})^p (y - \bar{y})^q ,$$

where $(\bar{x}, \bar{y}) = (\frac{1}{|R|}\sum_{(x,y)\in R} x, \frac{1}{|R|}\sum_{(x,y)\in R} y)$ and $|R|$ is the area of R. Then, as Figure 4, the orientation θ_R of R can be obtained using the equation:

$$\theta_R = arg \min_{\theta} \sum_{(x,y)\in R} \left[(x-\bar{x})\sin\theta - (y-\bar{y})\cos\theta \right]^2 . \quad (8)$$

More accurately, we get

$$\theta_R = \frac{1}{2}\tan^{-1}\left[\frac{2\mu_{1,1}}{\mu_{2,0}-\mu_{0,2}} \right]. \quad (9)$$

3.2 Edge descriptor

Not only vehicle color but also edge map of vehicle is used in this paper for orientation analysis. The difference of Gaussian (DOG) filter is used for extracting edge points. *DoG* is a wavelet function defined by

$$f(x,\sigma_1,\sigma_2) = \frac{1}{\sigma_1\sqrt{2\pi}}\exp(-\frac{x^2}{2\sigma_1^2}) - \frac{1}{\sigma_2\sqrt{2\pi}}\exp(-\frac{x^2}{2\sigma_2^2}) ,$$

where the σ_1 and σ_2 are the smooth operations. Then, similar to vehicle color feature, the log-polar location grid is used for vehicle classification.

3.3 Integration

Using the above descriptors, each query vehicle *x* has a forty-nine dimensional feature. Then, the *vehicle* descriptor of *x* is defined as

$$VD(x) = \{VC(x), E(x), \theta(x)\}, \quad (10)$$

where *VC(x)* is the vehicle color descriptor, *E(x)* is the edge map, and $\theta(x)$ is the vehicle color orientation. Assume that μ and Σ are the mean and variance of $VD(x)$, respectively. Then, given two vehicles *x* and *y*, their similarity be measured by this equation:

$$S(x,y) = \exp(-(VD(x)-\mu)\Sigma^{-1}(VD(y)-\mu)^t) . \quad (11)$$

4. Spectral clustering

After feature extraction, the spectral clustering algorithm will be used to cluster vehicles into eight orientations. Assume V is the vehicle database with *n* vehicles, i.e., $V = \{V_1, V_2, ..., V_n\}$. V can be further separated by a "cut" into two disjoint sets A and B, where $A \cup B = V$ and $A \cap B = \varnothing$. Similarity matrix is denoted by $S=\{ S_{ij} \}_{v_i, v_j \in V}$, where $S_{ij} = S_{ji} \geq 0$ is the similarity between V_i and V_j (see Eq.(11)). The total dissimilarity is:

$$cut(A,B) = \sum_{i\in A, j\in B} S_{ij}. \quad (12)$$

The *N-cut* clustering criterion for two classes is defined by

$$Ncut(A,B) = \frac{cut(A,B)}{assoc(A,V)} + \frac{cut(A,B)}{assoc(B,V)}, \quad (13)$$

where $assoc(A,V) = \sum_{i\in A, j\in V} S_{ij}$. Let D be the $N \times N$ diagonal matrix with $d_{ii} = \sum_{k=1}^{n} S_{ik}$, $i = 1,2,...,n$ on its diagonal, and W be a $N \times N$ symmetrical matrix with $W(i,j) = S_{ij}$. Then, we can bi-partition the data using the eigenvector with the second smallest eigenvalue solved from the generalized system,

$$(D-W)x = \lambda Dx. \quad (14)$$

Let $y = D^{1/2}x$. Eq.(14) can be then rewritten as

$$D^{-1/2}(D-W)D^{-1/2}y = \lambda y. \quad (15)$$

Based on the eigenvector, we can well categorize a vehicle into its suitable class of vehicle orientation.

5. Experimental results

To analyze the performance of our vehicle orientation detection algorithm, a database including 613 vehicle images was used in this paper for testing. For well testing our method, these images are captured under various situations, like contrast changes, complex background, lightings. To evaluate and measure the performances of our scheme to detect vehicle orientation, the precision is used in this paper. Precision is the ratio of correctly identified vehicle orientation $Num_{Correct}$ by the algorithm to the total vehicles number Num_{total} in database; that is,

$$Precision = Num_{Correct} / Num_{total} .$$

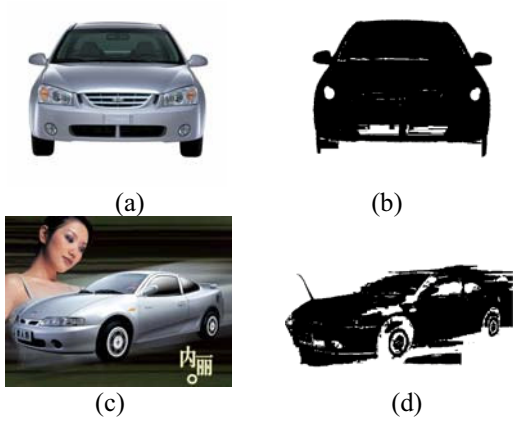

(a) (b) (c) (d)

Figure 5: Result of vehicle color detection. (a) Vehicle with simple background. (b) Result of (a). (c) Vehicle with complex background. (d) Result of (c).

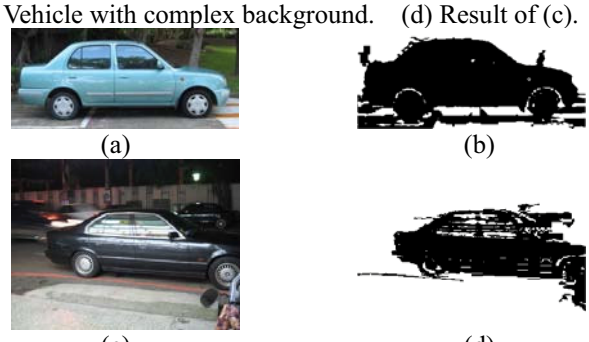

(a) (b) (c) (d)

Figure 6: Result of vehicle color detection. (a) and (b): Result of day time. (c) and (d): Result of evening time.

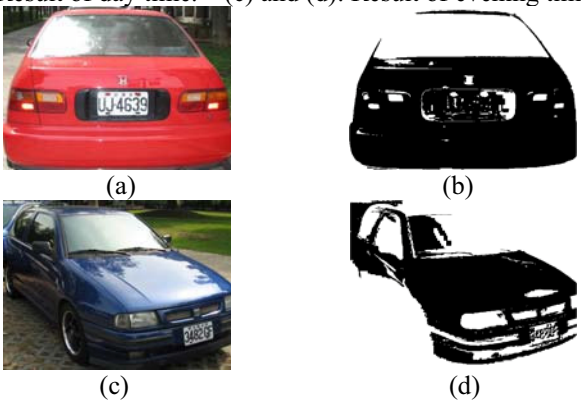

(a) (b) (c) (d)

Figure 7: Result of vehicle color detection. (a) Sunny day. (b) Result of (a). (c) Cloudy day. (d) Result of (c).

Figure 5 shows the result of vehicle color detection

under different backgrounds (simple or complex). Figure 6 shows the results of vehicle color detection when vehicles were captured under different time. In (c), even though the vehicle was captured under evening time, our proposed method still performed well to detect desired vehicle colors. Figure 7 shows the cases when vehicles were captured under different weather conditions. Figure 8 show the results of vehicle color classification under different image qualities. (a) shows a vehicle having high-contrast intensities. (c) is with lower contrast intensities. (e) shows the occlusion case. (b), (d), and (f) are, respectively, their corresponding results. Clearly, no matter what colors and situations a vehicle has, our proposed method works very well to detect all desired vehicle regions using our proposed color model.

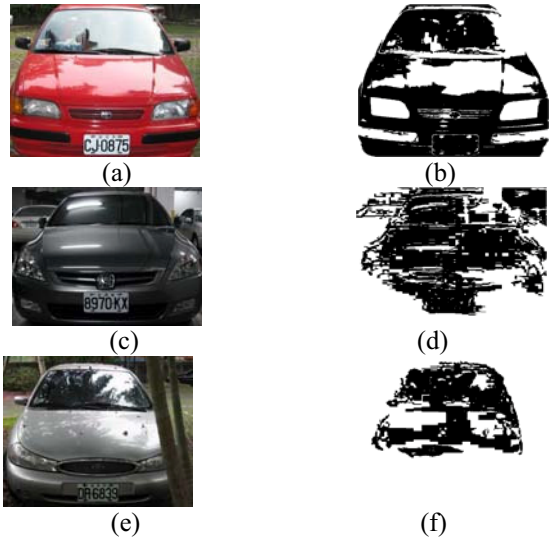

Figure 8: Result of vehicle color detection. (a) and (b): High contrast image. (c) and (d): Low contrast image. (e) and (f): Vehicle with occlusion.

Table 1: Accuracy analysis among different vehicle orientation categories.

Result	Front	Rear	R	L	FR	FL	RR	RL
Front	93	9	0	0	0	0	1	0
Rear	7	91	0	0	1	1	0	0
R	0	0	96	5	1	0	2	0
Left	0	0	4	95	0	1	0	2
FR	0	0	0	0	26	0	0	3
FL	0	0	0	0	0	65	2	0
RR	0	0	0	0	0	3	45	0
RL	0	0	0	0	2	0	0	58
Total	100	100	100	100	30	70	50	63
Accu.	93	91	96	95	86.7	92.9	90	92.1

Table 2. Precision analysis of vehicle orientation detection under different captured conditions.

Situations	Background		Weather		
	Simple	Complex	Sunny	Cloudy	Rainy
Precision	100	96	98	96.7	63
Situations	Lighting		Contrast		
	day	evening	High	Low	Occlusion
Precision	98	79.3	98	90	83

Table 1 lists the accuracy comparisons among different vehicle orientation categories, where R, L, FR, FL, RR, RL mean right, left, front-right, front-left, rear-right, and rear-let, respectively. The average accuracy of vehicle orientation detection using our proposed algorithm is 92.8%. Table 2 shows the precision analysis of vehicle orientation detection under different captured conditions. When vehicles were captured at day time, our system performs very well to recognize each vehicle orientation. According to the above experimental results, the superiority of the proposed method can be verified.

References

[1] O. k. Al-Shaykh and J. F. Doherty, "Invariant image analysis based on Radon transform and SVD," *IEEE Trans. on Circuits and Systems,* pp.123-133, Feb. 1996.

[2] D. Huawu and D. A. Clausi, "Gaussian MRF rotation-invariant features for image classification," *IEEE Trans. on PAMI,* vol.26, pp.951 - 955, July 2004.

[3] R. Cucchiara, M. Piccardi, and P. Mello, "Image analysis and rule-based reasoning for a traffic monitoring," *IEEE Trans. on ITS*, vol.1, no.2, pp.119-130, June 2002.

[4] G. L. Foresti, V. Murino, and C. Regazzoni, "Viehicle recognition and tracking from road imag sequences," IEEE Trans. on Vehicular Technology, vol.48, no.1, pp.301-318, Jan. 1999.

[5] V. Kastinaki, V. Zervakis, and K. Kalaitzakis, "A survey of video processing techniques for traffic applications," *Image and Vision Computing*, vol.21, no.4, pp.359-381, 2003.

[6] J. Wu, X. Zhang, and J. Zhou, "Vehicle detection in static road images with PCA-and- wavelet-based classifier," *IEEE of the international conference on ITS*, pp.740-744, 2001.

[7] Z. Sun, G. Bebis, and R. Miller, "On-road vehicle detection using Gabor filters and support vector machines," *IEEE International Conference on Digital Signal Processing*, vol.2, pp.1019-1022, 2002.

[8] M. Bertozzi, A. Broggi, and S. Castelluccio, "A real-time oriented system for vehicle detection," *Journal of Systems Architecture*, pp. 317-325, 1997.

[9] Y. Wang and H. Zhang, "Content-Based Image Orientation Detection with Support Vector Machines," *Proceeding of IEEE Workshop on CBAIVI*, pp.17-23, 2001.

[10] A. Vailaya, *et al*., "Automatic Image Orientation Detection," *IEEE Trans. on Image Processing*, vol. 11, no. 7, pp. 746-755, 2002.

[11] K. Mikolajczyk and C. Schmid, "Scale and affine invariant interest point detectors," *Proceeding of IJCV,* pp.63–86, 2004.

[12] L. W. Tsai, J. W. Hsieh, and K. C. Fan, "Vehicle Detection Using Normalized Color and Edge Map," *IEEE Inter. Conf. on IP*, vol.2, pp.598-601, 2005. (also to appear in *IEEE Transactions on IP*.)

[13] S. Belongie, J. Malik, and J. Puzicha, "Shape Matching and Object Recognition Using Shape Contexts," *IEEE Trans. on PAMI*, vol. 24, no. 4, pp. 509-522, Apr. 2002.

[14] J. Shi and J. Malik, "Normalized cuts and image segmentation," *IEEE Trans. on PAMI,* vol. 22, no.8, pp.888-905, August 2000.

[15] I. S. Dhillon, Y. Guan, and B. Kulis, "Kernel k-means, spectral clustering and normalized cuts," *Proceedings of International Conference on Knowledge Discovery and Data Mining*, pp. 551–556, Aug. 2004.

[16] R. Kannan, S. Vempala, and A. Vetta . "On clusterings-good, bad and spectral," Proceedings of Journal Annual Symposium on Foundations of Computer Science, pp.367-377, 2000.